Pergamon

SCIENCE DIRECT®

Bioorganic & Medicinal Chemistry Letters 13 (2003) 2173–2177

BIOORGANIC & MEDICINAL CHEMISTRY LETTERS

Potent Grb2–SH2 Domain Antagonists not Relying on Phosphotyrosine Mimics

Peng Li,[a] Manchao Zhang,[b] Ya-Qiu Long,[a,†] Megan L. Peach,[a] Hongpeng Liu,[b] Dajun Yang,[b] Marc Nicklaus[a] and Peter P. Roller[a,*]

[a]*Laboratory of Medicinal Chemistry, National Cancer Institute, National Institutes of Health, Frederick, MD 21702, USA*
[b]*School of Medicine, University of Michigan, Ann Arbor, MI 48109, USA*

Received 24 December 2002; accepted 1 April 2003

Abstract—Development of Grb2–SH2 domain antagonists is an effective approach to inhibit the growth of malignant cells by modulating Grb2-related Ras signaling. We report here potent Grb2–SH2 domain antagonists that do not rely on phosphotyrosine or its mimics. These non-phosphorylated antagonists were developed and further modified by constraining the backbone conformation and optimizing amino acid side chains of a phage library-derived peptide, **G1TE**. After extensive SAR studies and structural optimization, non-phosphorylated peptide **12** was discovered with an IC_{50} of 75 nM. This potent peptidomimetic provides a novel template for the development of non-pTyr containing Grb2-SH2 domain antagonists and acts as a chemotherapeutic lead for the treatment of erbB2-related cancer.

Src homology 2 (SH2) domains are characteristic families of conserved protein modules that mediate intracellular protein–protein interactions.[1] Among these SH2 domains, the Grb2–SH2 domain directly mediates the activation of mitogenic Ras pathway. An aberrant Grb2-dependent Ras activation pathway has been shown to be essential for cellular transformation in a subset of human tumors.[2,3] Overexpression of Grb2 protein is also related to liver tumorigenesis in mice[4] and human breast cancer cells.[5] Therefore, development of Grb2–SH2 domain antagonists is an effective approach to block the growth of malignant cells.[6]

The binding of SH2 domains to target proteins in cells involves the recognition of a phosphotyrosine residue, and a specific sequence motif flanking the phosphorylated tyrosine residue.[7] Because of the decisive role of phosphotyrosine in binding and the similarity of SH2 domains, specificity becomes an inevitable concern in the process of Grb2–SH2 domain antagonist design. The traditional affinity-based drug design and screening may develop potent inhibitory ligands, but with low specificity under these circumstances.[8]

Considering both affinity and specificity concerns, our collaborators developed a phage-display library screening strategy, and discovered a disulfide-bridged cyclic decapeptide, termed **G1**, from 10^7 different sequences.[9] This non-phosphotyrosine containing cyclopeptide specifically binds to the Grb2–SH2 domain, but does not bind to the homologous Src–SH2 domain. Apparently, the absence of a phosphate moiety in this phage peptide contributes to its remarkably high specificity. This encouraging discovery lead us to the design of non-pTyr containing Grb2–SH2 domain antagonists based upon **G1** and its thioether-bridged analogue **G1TE**.[10,11] In this article, we report our most recent findings for the design and synthesis of non-phosphorylated Grb2–SH2 domain antagonists.

The thioether-bridged cyclic peptide ligands were synthesized using the procedure described previously.[10] The linear peptide precursors were synthesized on an ABI 433A peptide synthesizer, starting with Fmoc-PAL resin for establishing the C-terminal carboxamide, and using the chemical protocols based on the Fmoc chemistry. The 'difficult' coupling steps were carried out manually, and coupled twice using HATU as the coupling reagent.

*Corresponding author. Tel.: +1-301-846-5904; fax: +1-846-6033; e-mail: proll@helix.nih.gov
†Current address: Shanghai Institute of Materia Medica, Chinese Academy of Sciences, Shanghai 200031, China.

0960-894X/03/$ - see front matter © 2003 Elsevier Science Ltd. All rights reserved.
doi:10.1016/S0960-894X(03)00385-8

The oxidation of the thioether functionality into sulfoxide was accomplished using a 5% H_2O_2 aqueous solution. The resulting two isomers were easily separated by RP-HPLC. CD spectra of peptides (0.1 mM) in 10 mM phosphate buffer (pH 7.2) were recorded on a JASCO-715 spectropolarimeter, and represent average values from four scans. The resulting spectra were baseline corrected and smoothed.

An N-terminally biotinylated phosphopeptide, biotin-DDPSpYVNVQ, encompassing the Grb2 SH2 domain binding sequence derived from SHC protein, was bound at 20 ng/mL to 96-well plates overnight. Nonspecific interactions were inhibited by blocking with 5% bovine serum albumin containing TBS. Recombinant purified Grb2 SH2–GST fusion protein and samples with serial dilutions were incubated for at least 2 h. After extensive washing with 0.1% bovine serum albumin in TBS, bound Grb2 SH2 domain was detected using anti-GST antibodies and goat anti-mouse antibody conjugated to alkaline phosphatase. Quantitation of bound alkaline phosphatase was achieved by a colorimetric reaction employing *para*-nitrophenyl phosphate as substrate. Each compound was subjected to a minimum of three determinations. Assays were conducted with a positive control of known potency, with additional controls being performed without peptide or protein.

Simulations were performed with the Insight II 2000/Discover 97 modeling package, with the cff91 forcefield. Models were constructed based on our structure for the cyclic peptide G1TE, which was built, as described previously,[10] from the X-ray crystal structure of the KPFpYVNV peptide bound to the Grb2–SH2 domain.[12] For refinement, the peptide-receptor complex first underwent 50 steps of steepest descent and 150 steps of conjugate gradient minimization. Harmonic positional restraints on the backbone atoms were gradually relaxed over the course of the minimization to eliminate any steric clashes in the side chains without inducing deformations in the backbone. Next, the complex was solvated with a layer of water molecules 25 Å thick over the binding site area, and equilibrated briefly with ten molecular dynamics runs of 200 steps each at 300 K. Velocities were reassigned to a random Boltzmann distribution for each run. During dynamics all atoms were held fixed except for the peptide, binding site residues within 5 Å of the peptide, and the inner 15 Å of the water layer. The final structure was then minimized for 300 steps with the conjugate gradient algorithm.

It is known that the two negative charges on the phosphate group of phosphotyrosine at physiological pH can substantially impair cell membrane penetration. In addition, the possible hydrolysis of the phosphate ester bond by phosphatases is another drawback of the traditional pTyr-containing Grb2–SH2 domain inhibitors. Therefore, our goal is to develop non-phosphorylated Grb2–SH2 domain antagonists, based upon the lead peptide **G1TE**. In our previous studies,[10,13] we have demonstrated the functional significance of the amino acids in positions 1 and 3. Besides these two amino acid residues, the amino acids in positions 4, 5, 6, and 9 of **G1TE** analogues also have interactions with the Grb2 protein, as shown in Figure 1. Therefore, we designed and synthesized a series of **G1TE** analogues by modifying the side chains of the amino acid residues in these positions, and constraining the backbone conformation (Fig. 1).

We find that the Grb2–SH2 domain requires the phosphopeptide ligand to bind to it in a unique β-turn fashion, due to the existence of Trp121 near the asparagine binding pocket of the SH2 domain.[12] Therefore, we assume that introducing a turn-inducing amino acid in position 4 of **G1TE** analogues may favorably influence binding affinity. As shown in Table 1, the binding affinity was indeed remarkably improved when replacing Glu4 with Pro4 (**1** vs **2**). Since the acidic side chain of Glu4 of **G1TE** was observed to have interactions with Ser141 and Arg142 of the Grb2–SH2 domain as indicated by molecular modeling, we incorporated the amino acid Adi, the side chain of which is one carbon longer than glutamic acid, in position 4 to improve this charge interaction. Unfortunately, the binding affinity of peptide **4** was not enhanced compared to peptide **3**, probably due to the entropic penalty caused by the increased side chain flexibility. However, the inhibitory activity was improved by incorporating a C_α,C_α-disubstituted amino acid, such as Ach and BCH, in position 4. When replacing Glu4 with Ach4, the resulting peptide **6** loses charge interactions with Ser141 and Arg142, but gains hydrophobic Van der Waals interactions with Gln106 and Phe108 of the Grb2-SH2 domain. In addition, the 3_{10} helix turn, with the torsion angles $\Phi = -62.1°$, $\Psi = -34.3°$ and $\omega = 170.4°$, induced by Ach is also favored for the peptide binding to the Grb2–SH2 domain. The overall effect makes peptide **6** approx. 2-fold more potent than peptide **3** (Table 1).

Besides the functional significance of the amino acid in the 1-, 3-, 4-, and 5-positions, which have extensive interactions with the binding cavity of Grb2-SH2 domain, the amino acid in position 8 also plays an important role for the effective binding of **G1TE** analogues to Grb2 protein. When Met8 is replaced with alanine, the inhibitory activity of the resulting analogue decreases 60-fold.[11] Interestingly, the 8th amino acid residue of the **G1TE** analogue has no interactions with Grb2–SH2 domain, as indicated by our molecular modeling (Fig. 2). However, the hydrophobic packing of Met8, Leu2, Cys10, and the *N*-acetyl group stabilizes the favored conformation for other residues binding to Grb2–SH2 domain. Considering these characteristic interactions, we incorporated a series of hydrophobic amino acids in position 8, as shown in Table 2. The binding affinity of the modified peptides **8**, **10** and **11** increases approximately 2-fold when replacing Met8 with pentafluorophenylalanine (F_5Phe), 2-naphthylalanine (2-Nal) or neopentylglycine (NPG). Compared to methionine, these unnatural amino acids are more hydrophobic and less flexible, which results in favorable and well defined Van der Waals interactions with Leu2 and Cys10, as shown in Figure 2. However, these improved Van der Waals interactions can be overweighed by increasing exposed hydrophobic surface

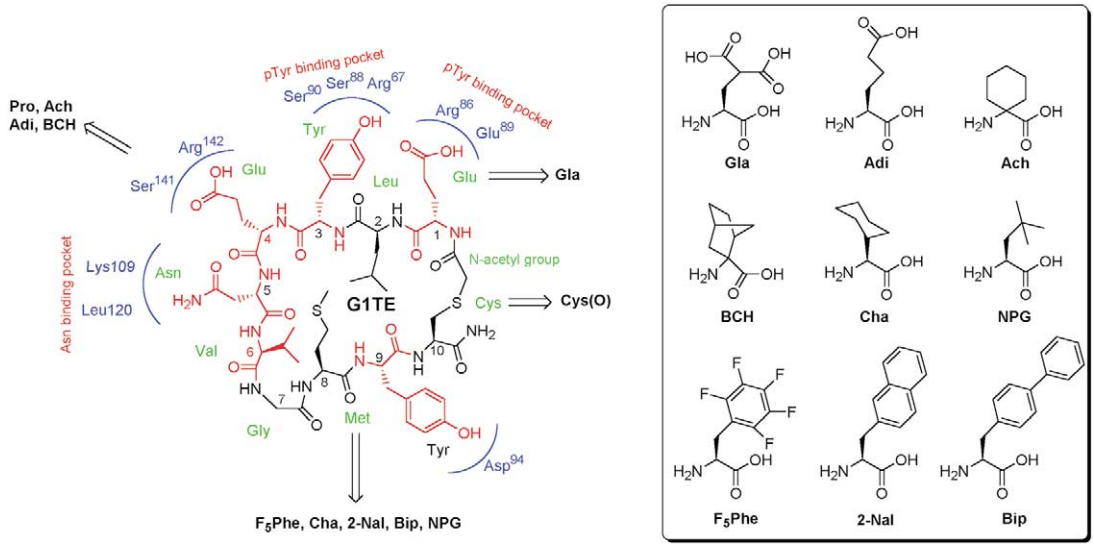

Figure 1. Interactions of phage library derived **G1TE** with the Grb2–SH2 domain and design of Grb2–SH2 domain antagonists. The amino acid residues colored in red were found to have interactions with the blue-colored amino acid residues of Grb2–SH2 domain. The structures of the incorporated unnatural amino acids are listed on the right-side panel.

Table 1. Potentiating effect of incorporation of turn inducing amino acids in position 4 of **G1TE** analogues[a]

Compd	Peptide sequence description	Activity IC_{50}, μM[b]
1	**G1TE**	>100[c]
2	G1TE(**Pro**^{4})	7.83 (±0.63)
3	G1TE(Gla^1)	0.991 (±0.095)
4	G1TE(Gla^1**Adi**^{4})	1.51 (±0.21)
5	G1TE(Gla^1**BCH**^{4})	0.730 (±0.340)
6	G1TE(Gla^1**Ach**^{4})	0.525 (±0.017)

[a]The binding affinity of these compounds was evaluated by ELISA assays.
[b]Values are means of at least three experiments, standard deviation is given in parentheses.
[c]Biacore assay indicates that **G1TE** exhibits inhibitory activity with an IC_{50} = 20 μM.[13]

area under some circumstances. For instance, the binding affinity of the resulting peptides **9** was not improved, and even decreased when Met8 was substituted with biphenylalanine (Bip).

To further constrain the backbone conformation of G1TE analogues, we also tried to modify the thioether bridge of these peptides, since this –CH_2–S–CH_2– motif is conformationally flexible and may contribute to an entropic penalty for the thioether-bridged **G1TE** analogue binding to Grb2 protein. As we expected, the inhibitory activity of the peptide was improved when oxidizing the flexible thioether linkage into the relatively rigid sulfoxide linkage, as shown in Table 2. Interestingly, only one of the two sulfoxide analogues is more active, the other diastereoisomer is less active than the corresponding thioether peptide. For instance, the sulfoxide **12** is 3 times more potent than the thioether analogue **11**, while the other sulfoxide isomer **13** is 3-fold less active than **11** and 10-fold less active than **12** (Table 2). To determine the absolute configuration of the two sulfoxide isomers, we compared the CD spectra of these peptides. Subtracting the CD spectra of the two diastereomeric sulfoxide isomers, **12** and **13** from the

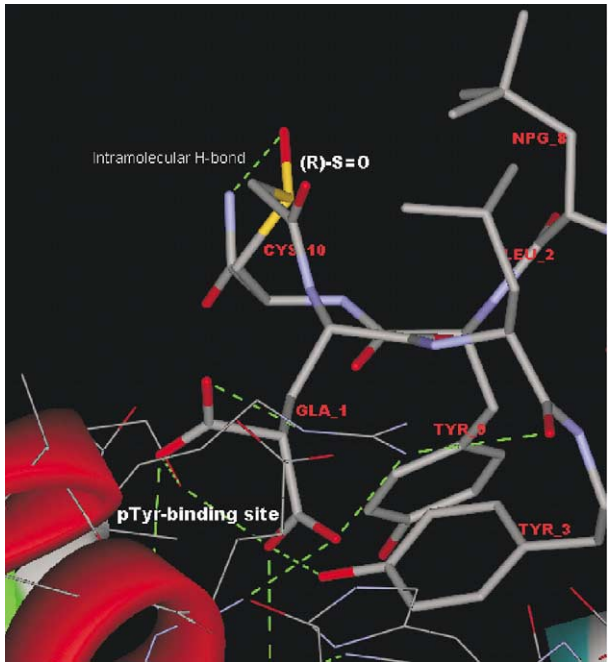

Figure 2. Interactions of peptide **12** (presented in stick style) with the Grb2–SH2 domain (with side chain residues presented in thin line style). Protein backbone is shown with solid ribbon. Green dotted lines represent H-bonds.

thioether **11**, respectively, provides us with the net influence of the sulfoxide configuration on the spectra, as shown in Figure 3. The general guidelines for the determination of the absolute configuration of cysteine sulfoxide derivatives has been well documented.[14–17] A negative cotton effect, centered at the S(O) absorption band around the 220 nm region, correlates with an *R* configuration, whereas a positive cotton effect correlates with an *S* configuration. Therefore, we can assume that the sulfoxide group of peptide **12** adopts an *R* configuration deduced from its negative cotton effect around 220 nm region (Fig. 3). Accordingly, peptide **13** adopts an *S*

Table 2. Modification of the thioether linkage and the amino acid in position 8 of **G1TE** ($Gla^1Ach^4AA^8AA^{10}$) analogues[a]

Compd[b]	Amino acid composition		Activity IC_{50}, μM[c]
	AA^8	AA^{10}	
6	Met	Cys	0.525 (±0.017)
7	Cha	Cys	0.815 (±0.330)
8	2-Nal	Cys	0.271 (±0.013)
9	Bip	Cys	0.502 (±0.104)
10	F_5Phe	Cys	0.238 (±0.007)
11	NPG	Cys	0.244 (±0.045)
12	NPG	Cys(O)-(*R*)	0.0746 (±0.0037)
13	**NPG**	Cys(O)-(*S*)	0.747 (±0.180)
14	2-Nal	Cys(O)-(*R*)	0.314 (±0.124)
15	**2-Nal**	Cys(O)-(*S*)	4.86 (±2.70)
16	**Cha**	Cys(O)-(*R*)	0.149 (±0.083)
17	**Cha**	Cys(O)-(*S*)	1.41 (±0.42)

[a]The binding affinity of these compounds was evaluated by ELISA assays.
[b]General sequence of these peptides is **G1TE**($Gla^1Ach^4AA^8AA^{10}$). The structures of the unnatural amino acids and peptides are shown in Figure 1.
[c]Values are means of at least three experiments; standard deviation is given in parentheses.

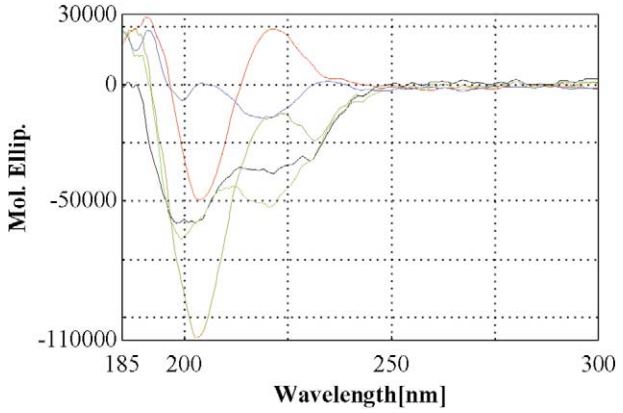

Figure 3. CD spectra of peptide **11** (black), **12** (green), and **13** (brown). The derived spectrum by the subtraction of the CD spectrum of peptide **12** from **11** is shown as blue solid line. The red solid line is the result of the subtraction of the CD spectrum of peptide **13** from **11**.

configuration, as indicated by the positive cotton effect around 220 nm, when compared to the precursor thioether peptide **11**. These results can be further confirmed by molecular modeling, and thus well correlate with their inhibitory activity. The *R*-configured peptide **12** essentially adopts a similar conformation to the thioether peptide **11**, and the S=O group forms an intramolecular hydrogen bond with the *C*-terminal amide, indicated by molecular modeling (Fig. 2). Consequently, the enhanced molecular rigidity greatly reduces the entropic penalty in the process of binding, which leads to the increased potency of peptide **12**. The similarity of the conformations of peptides **11** and **12**, can also be observed form their CD spectra. Other than the absorption band caused by sulfoxide around 220 nm, the CD spectra of the two peptides are very similar, as shown in Figure 2. However, the conformations of peptide **13** and **11** are quite different. Peptide **13** exhibits a much stronger negative cotton effect in the amide bond absorption region around 205 nm. Molecular modeling suggests that peptide **13** concessively undergoes a conformational change due to repulsion between the oxygen of the *S*-configured sulfoxide and the carbonyl oxygen of the *N*-acetyl group. In the *S*-configuration, the sulfoxide oxygen also disrupts the hydrophobic packing between residue 8 and the *N*-acetyl group. This unfavorable conformational change makes peptide **13** 10 times less active than its isomer, peptide **11**. This trend was also observed in the Cha8-containing peptides **7**, **16** and **17**. Compared to thioether-bridged **G1TE** analogues, these sulfoxide-bridged cyclopeptides prefer a relatively less bulky amino acid, such as NPG and Cha, in position 8. When oxidizing the 2-Nal8-containing thioether peptide **8** into sulfoxide, the activities of the resulting peptides **14** and **15** are not improved comparing to their thioether analogue, due to the steric hindrance caused by the bulky side chain of 2-naphthylalanine.

A series of potent non-pTyr containing Grb2-SH2 domain antagonists was designed and synthesized based upon the phage library derived **G1TE**. According to our extensive SAR studies, we found that a turn-inducing amino acid, such as Ach and BCH, is preferred in position 4, due to characteristic β-turn binding conformation required by the Grb2–SH2 domain. Incorporation of a hydrophobic amino acid, such as F_5Phe, 2-Nal and NPG, in position 8 can further improve the binding affinity of **G1TE** analogues because the hydrophobic packing within amino acid residues in the 8-, 2-, and 10-positions stabilizes the favored binding conformation of these peptide ligands. Oxidation of the thioether linkage into sulfoxide also improves the binding affinity of these cyclic peptides due to the favorable constraint of backbone conformation. Based upon these findings, we discovered a very potent non-phosphorylated Grb2–SH2 domain antagonist **12**, with an IC_{50} of 75 nM. Since this potent cyclic peptidomimetic does not possess the phosphate group or contain a pTyr mimic, it may exhibit better pharmacokinetic properties and specificity than pTyr-containing inhibitors, and provides us with a novel template for the development of chemotherapeutic agents targeting Grb2 protein for the treatment of cancer caused through erbB2 overexpression.

References and Notes

1. Sawyer, T. K. *Biopolymers* **1998**, *47*, 243.
2. Xie, Y.; Pendergast, A. M.; Hung, M. C. *J. Biol. Chem.* **1995**, *270*, 30717.
3. Tari, A. M.; Hung, M. C.; Li, K.; Lopez-Berestein, G. *Oncogene* **1999**, *18*, 1325.
4. Diwan, B. A.; Ramakrishna, G.; Anderson, L. M.; Ramljak, D. *Toxicol. Pathol.* **2000**, *28*, 548.
5. Yip, S. S.; Daly, R. J. *Int. J. Cancer* **2000**, *88*, 363.
6. Gay, B.; Suarez, S.; Caravatti, G.; Furet, P.; Meyer, T.; Schoepfer, J. *Int. J. Cancer* **1999**, *83*, 235.
7. Anderson, D.; Koch, C. A.; Grey, L.; Ellis, M. F.; Pawson, T. *Science* **1990**, *250*, 979.
8. Kessels, H. W. H, Ward, A. C., Schumacher, T. N. M. *Proc. Natl. Acad. Sci. USA*. **2002**, *99*, 8524.
9. Oligino, L.; Lung, F.-D. T.; Sastry, L.; Bigelow, J; Cao, T.; Curran, M.; Burke, T. R.; Wang, S.-M.; Krag, D.; Roller, P. P.; King, C. R. *J. Biol. Chem.* **1997**, *272*, 29046.
10. Long, Y.-Q.; Voigt, J. H.; Lung, F.-D. T.; King, C. R.; Roller, P. P. *Bioorg. Med. Chem. Lett.* **1999**, *9*, 2267.

11. Lung, F.-D. T.; Long, Y.-Q.; King, C. R.; Varady, J.; Wu, X.-W.; Wang, S.; Roller, P. P. *J. Peptide Res.* **2001**, *57*, 447.
12. Rahuel, J.; Gay, B.; Erdmann, D.; Strauss, A.; Garcia-Echeverria, C.; Furet, P.; Caravatti, G.; Fretz, H.; Schoepfer, J.; Grutter, M. *J. Nat. Struct. Biol.* **1996**, *3*, 586.
13. Long, Y.-Q.; Yao, Z.-J.; Voigt, J. H.; Lung, F.-D. T.; Luo, J. H.; Burke, T. R.; King, C. R.; Yang, D.; Roller, P. P. *Biochem. Biophys. Res. Commun.* **1999**, *264*, 902.
14. Ottenheijm, H. C. J.; Liskamp, R. M. J.; Helquist, P.; Lauher, J. W.; Shekhani, M. S. *J. Am. Chem. Soc.* **1981**, *103*, 1720.
15. Kubec, R.; Musah, R. A. *Phytochemistry* **2001**, *58*, 981.
16. Van den Broek, L. A. G. M.; Breuer, M. L.; Liskamp, R. M. J.; Ottenheijm, H. C. J. *J. Org. Chem.* **1987**, *52*, 1511.
17. Liskamp, R. M. J.; Zeegers, H. J. M.; Ottenheijm, H. C. J. *J. Org. Chem.* **1981**, *46*, 5408.